

Categorical Quantum Circuits

Ville Bergholm^{1,*} and Jacob D. Biamonte^{2,†}

¹*Department of Applied Physics, Aalto University School of Science and Technology*

²*Oxford University Computing Laboratory*

The aim of this work is to bring the fields of category theory and quantum information science into closer contact. Specifically, we present an explicit representation of dagger compact closed categories in terms of an extended form of quantum circuit diagrams, which we have used to produce results new to both areas. We map the string diagram calculus previously used in the categorical axiomatization of quantum mechanics onto quantum circuits. This approach introduces a set of tools for manipulating and simplifying circuits of systems of arbitrary dimension in novel, powerful ways, while remaining within a model that is directly and easily applicable to problems stated in the language of quantum information science. The circuit diagrams themselves now become morphisms in a category, making quantum circuits a special case of a much more general mathematical framework. To ease the reader into the subject, we have strived to present these ideas in a way that does not require a category theory background. All the main proofs we give use only standard linear algebra techniques.

PACS numbers: 03.65.Fd, 03.65.Ca, 03.65.Aa

Keywords: category theory, quantum circuit model

*ville.bergholm@iki.fi

†jake@qubit.org

I. INTRODUCTION

This work aims to extend the diagrammatic methods commonly used with the almost ubiquitous quantum circuit model (QCM). The quantum circuit model was put into its current form in the pioneering work by Yao [1] which built on several other notable results including those by Deutsch. It has remained largely unchanged from this original formulation up to the present day, with perhaps the first exception being due to the early work by Aharonov, Kitaev and Nisan [2] who, in their formulation, replace pure states with state operators and unitary gates with completely positive maps. This overcomes several limitations of the standard QCM, such as representing measurements in the middle of the computation, decoherence, and probabilistic subroutines.

Diagrammatic methods in physics and in quantum information science have a long history [3–5]. Building on the results of reversible logic and computation, perhaps the first to note their importance in quantum information science was David Deutsch. The importance of diagrammatic methods stems from the fact that they enable one to perform mathematical reasoning and even actual calculations using intuitive graphical objects instead of abstract mathematical entities. Modern quantum circuit diagrams (QCDs) are highly sophisticated tools, even though many of their features were developed in a largely ad hoc manner.

Our work approaches the problem of developing diagrammatic methods from the direction of category theory but also employs ideas of tensor network theory and related concepts. Category theory is often used as a unifying language for mathematics, and in more recent times to formulate physical theories [6, 7]. One of the strong points of the area of applied mathematics known as categorical modeling is that it comes equipped with a powerful graphical language that can be proven to be fully equivalent to the corresponding algebraic notation. Because of this, one sometimes hears the statement “Category theory formally justifies its absence”.

Category theory has only recently been used to model quantum mechanics [8]. Connecting categorical methods to the established area of quantum circuit theory seems reasonable as category theory provides the exact arena of mathematics concerned with the diagrammatic reasoning present in the existing methods to manipulate quantum circuits. These *string diagrams* capture the mathematical properties of how maps (states and operators in the circuit model) can be composed. By considering the categorical description of the mathematics used in quantum mechanics, one essentially gets quantum circuits for free!

Traditional QCDs are graphs that are planar and directed acyclic. These are a subclass of the graphs one can construct in a compact closed category. One can go beyond this by considering the symmetric, compact structure of the category. This amounts to adding in maps that are equivalent to Bell states and Bell effects: one can then arrive e.g. at the well known results surrounding channel-state duality. However, categorical dualities [8] come with something novel: an intuitive graphical interpretation which we use to manipulate quantum circuits in new ways and which exposes channel-state duality as a consequence of simply bending wires. For instance, by temporarily dropping causality (directed temporal ordering) one can with relative ease perform very nontrivial operations on the diagrams and then convert them back into a standard, physically implementable quantum circuits.

The categorical model of quantum theory makes rigorous several diagrammatic notations. Unfortunately its range of applicability to problems in quantum information science has lacked as the focus has been mainly on purely mathematical results. The current approach relies on a reduced set of the operations and identities present in the traditional quantum circuit (and more generally, quantum network) model. On the other hand, the circuit model does not exploit some of the elegant mathematical ideas appearing in category theory.

Both category theory and the quantum circuit model are well developed fields, backed by years of fundamental research and an increasing number of publications. The state of the art in graphical languages used in quantum information science can be found e.g. in [9]. We also note the work in [10]. As in the theory of tensor network states [9], the theory of categories allows one to study the mathematical structure formed by the composition of processes themselves (see for instance work on tensor network states [11]).

Our main focus in this article is to connect these two fields: the mathematical ideas appearing in category theory with the state of the art in quantum information science. By showing how the structure of a dagger compact closed category can be represented in a quantum circuit, and by showing how quantum circuits can be transformed using methods from category theory we aim to derive results useful to both areas.

Background reading

This work attempts to be mostly self contained. For those interested in the string diagrams, Selinger’s “Survey of graphical languages for monoidal categories” offers an excellent starting place [12]. The mathematical insight behind using pictures to represent these and related networks dates back to Penrose and in quantum circuits, to Deutsch. The mathematics behind category theory is based largely on a completeness result (originally proved by Joyal and Street) about the kinds of string diagrams we consider here (and actually the Kelly-Laplaza-Selinger coherence result) [12–14].

We build on ideas across several fields. This includes the work by Lafont [15] which was aimed at providing an algebraic theory for classical Boolean circuits. Lafont’s work is related to the more recent work on proof theory by Guiraud [16]. By considering quantum protocols, Samson Abramsky and Bob Coecke provided a categorical framework which they later called “Categorical quantum mechanics” [8]. A good deal of work built on different aspects of their model. In particular, by considering quantum observables related by Hadamard transforms, Bob Coecke and Ross Duncan made progress towards a categorical model of quantum theory applicable to problems in quantum information and computation [17].

Recently several tutorials on categories and the corresponding diagrammatic calculus have been made available. These include the survey [6], the more specialized paper [18] and the light read [19].

II. CATEGORIES

In this section we will sketch the basic concepts and definitions that surround the present work for the benefit of readers unfamiliar with category theory, in a way that we hope appeals to researchers working on quantum information theory. We will skim over details not essential to the present study. In particular, this will include several of the more technical points of these structures such as natural isomorphisms and coherence axioms. For a more complete treatment of the subject, see e.g. [12].

Definition 1 (Category). A *category* \mathcal{C} is an algebraic structure that consists of

1. $\text{ob}(\mathcal{C}) = \{A, B, C, \dots\}$, a class of *objects*.
2. $\text{hom}(\mathcal{C})$, a class of *morphisms* (sometimes called arrows), that is, maps between the objects. We use

$$\text{hom}_{\mathcal{C}}(A, B) = \{f \mid f : A \rightarrow B, A, B \in \text{ob}(\mathcal{C})\} \subset \text{hom}(\mathcal{C}) \quad (1)$$

to denote the class of all morphisms from A to B in the category.

3. *compositions* of morphisms, i.e., for every triple of objects A, B, C , the binary operation

$$\circ : \text{hom}_{\mathcal{C}}(B, C) \times \text{hom}_{\mathcal{C}}(A, B) \rightarrow \text{hom}_{\mathcal{C}}(A, C). \quad (2)$$

Furthermore, the components of \mathcal{C} must fulfill the following axioms:

- (i) Associativity of composition: $(h \circ g) \circ f = h \circ (g \circ f)$ holds for all morphisms $f \in \text{hom}_{\mathcal{C}}(A, B)$, $g \in \text{hom}_{\mathcal{C}}(B, C)$, $h \in \text{hom}_{\mathcal{C}}(C, D)$.
- (ii) Existence of identity morphisms: For each object $A \in \text{ob}(\mathcal{C})$ there is an identity morphism $1_A \in \text{hom}_{\mathcal{C}}(A, A)$ such that for every morphism $f \in \text{hom}_{\mathcal{C}}(A, B)$ we have $1_B \circ f = f \circ 1_A = f$. (It can readily be shown that the identity morphisms are unique.)

An *isomorphism* is an invertible morphism. The map $f \in \text{hom}_{\mathcal{C}}(A, B)$ is an isomorphism iff $\exists g \in \text{hom}_{\mathcal{C}}(B, A)$ for which $g \circ f = 1_A$ and $f \circ g = 1_B$. This makes f and g each others’ inverses: $g = f^{-1}$.

We will build on this basic definition in several key stages. The first is the notion of a strict monoidal category. A *strict monoidal* category is a category equipped with an associative *tensor product* \otimes . It is a bifunctor, i.e. a binary operation defined for both the objects and the morphisms, which preserves the relationship between them, and has a unit object $\mathbf{1} \in \text{ob}(\mathcal{C})$ such that for any object A we have $A \otimes \mathbf{1} = A = \mathbf{1} \otimes A$.

Adding a family of *natural symmetry isomorphisms* $c_{A,B} : A \otimes B \rightarrow B \otimes A$ with the property $c_{B,A} \circ c_{A,B} = 1_A \otimes 1_B$ makes a monoidal category *symmetric*. Intuitively the symmetry isomorphisms mean that the relative order of the objects in a tensor product carries no fundamental significance.

A *compact closed* category is a symmetric monoidal category in which for each object $A \in \text{ob}(\mathcal{C})$ there is a *dual object* $A^* \in \text{ob}(\mathcal{C})$, and the *unit* and *counit* morphisms $\eta_A : \mathbf{1} \rightarrow A^* \otimes A$ and $\epsilon_A : A \otimes A^* \rightarrow \mathbf{1}$, which fulfill the adjunction triangle equations

$$(\epsilon_A \otimes 1_A) \circ (1_A \otimes \eta_A) = 1_A, \quad (3)$$

$$(1_{A^*} \otimes \epsilon_A) \circ (\eta_A \otimes 1_{A^*}) = 1_{A^*}. \quad (4)$$

In a sense the unit and counit morphisms correspond to entangled states.

Finally, a *dagger* compact closed category is a compact closed category that comes equipped with the *dagger functor* [8], which captures the notion of adjoint. It is an involution that associates every morphism $f : A \rightarrow B$ with its *adjoint* morphism $f^\dagger : B \rightarrow A$, and is compatible with both the composition and the tensor product. The dagger functor behaves precisely in the way one would expect from the Hermitian adjoint operation on a Hilbert space. To make the analogy even stronger, an isomorphism $f : A \rightarrow B$ is said to be *unitary* iff $f^\dagger = f^{-1}$.

III. EXTENDED QUANTUM CIRCUIT DIAGRAMS

We will now begin our presentation of an extended form of the existing diagrammatic notation for describing quantum circuits. Some of these concepts were first introduced in [8, 17, 20], where the authors derived a categorical representation that was expressive enough to represent many of the components used in standard quantum circuits. In a seemingly independent research track, some of these concepts also appeared in [9, 10] as well as related work.

Each extended quantum circuit diagram corresponds to a single morphism in the category QC. The main difference to ordinary QCDs is that an extended diagram *does not have to correspond to a quantum operation*. One of the key benefits of these diagrams is that they can be manipulated in a very intuitive, visual way. Objects (boxes etc.) on wires can be slid along them. The wires themselves can be bent and rearranged. Nodes where several wires meet can often be combined and split according to simple rules. After such changes, the diagram can be converted back into an ordinary, physically implementable quantum circuit, depending on the specific application.

Definition 2 (The category of quantum circuits QC). QC is a category that consists of

1. Objects $A := \{\mathcal{A}, D_A\}$, where $\mathcal{A} = \mathcal{A}_1 \otimes \mathcal{A}_2 \otimes \dots \otimes \mathcal{A}_{n_A}$ is a finite dimensional complex Hilbert space and $D_A = (d_{A_i})_{i=1}^{n_A}$ a list of positive integer dimensions such that $\dim \mathcal{A}_i = d_{A_i}$. n_A denotes the number of *subsystems* in the object. If $n_A = 1$ the object is *simple*, otherwise it is *composite*.
2. Morphisms $f : A \rightarrow B$, bounded linear maps between the Hilbert spaces \mathcal{A} and \mathcal{B} . D_A and D_B are the input and output dimensions of the morphism, respectively.
3. Composition of morphisms \circ , which is just the usual composition of linear maps.
4. Tensor product bifunctor \otimes with the unit object $\mathbf{1} := \{\mathbb{C}, (1)\}$. $A \otimes B := \{\mathcal{A} \otimes \mathcal{B}, D_A \star D_B\}$, where \star denotes list concatenation with the elimination of unnecessary singleton dimensions, and $f \otimes g$ is the usual tensor product of linear operators.¹
5. Dagger functor \dagger , which is identity on the objects and takes the Hermitian adjoint of the morphisms.
6. Dual functor $*$, which is identity on the objects and takes the transpose of the morphisms in the computational basis. The unit and counit morphisms are likewise defined in terms of the computational basis: $\eta_A = \sum_k |k, k\rangle_{\mathcal{A} \otimes \mathcal{A}}$, $\epsilon_A = \eta_A^\dagger$.

Theorem 3. QC is a dagger compact closed category

Proof Sketch.

- It is straightforward to show that QC is a category: composition of the morphisms is clearly associative, and for each object A the corresponding identity morphism 1_A is the identity map $\mathbb{1}_{\mathcal{A}}$ on \mathcal{A} .

¹ Note that the same symbol \otimes is used to denote three different but related things: (1) the categorical tensor product bifunctor of objects and morphisms, (2) the tensor product of vector spaces and (3) the tensor product of linear operators.

- QC is also readily seen to be strictly monoidal. The tensor product is associative, fulfills the bifunctor requirements $(g \circ f) \otimes (t \circ s) = (g \otimes t) \circ (f \otimes s)$ and $1_A \otimes 1_B = 1_{A \otimes B}$, and $1 \otimes A = A \otimes 1 = A$. The associator and left and right unitor isomorphisms are thus given by $\alpha_{ABC} = \mathbb{1}_{A \otimes B \otimes C}$ and $\lambda_A = \rho_A = \mathbb{1}_A$. The pentagon and triangle coherence axioms are trivially fulfilled.
- The symmetric braiding isomorphism $c_{A,B} : A \otimes B \rightarrow B \otimes A$, required to make QC symmetric monoidal, is given by the SWAP gate: $c_{A,B} := \text{SWAP}_{A,B} := \sum_{ab} |ba\rangle_{B \otimes A} \langle ab|_{A \otimes B} = c_{B,A}^{-1}$ which fulfills the hexagon axiom.
- The dagger is a contravariant endofunctor, is easily seen to be involutive ($f^{\dagger\dagger} = f$) and has the proper interaction with the composition and tensor product: $1_A^\dagger = 1_A$, $(g \circ f)^\dagger = f^\dagger \circ g^\dagger$, and $(f \otimes g)^\dagger = f^\dagger \otimes g^\dagger$. Furthermore, the morphisms α , λ , ρ and c are all unitary so QC is dagger symmetric monoidal.
- The dual is also a contravariant endofunctor and the unit and counit morphisms fulfill the adjunction triangles (“snake equations”), and are symmetric. Together with the other properties this makes QC a dagger compact closed category.

□

A unitary QC-morphism is also called a *gate*.

Remark 4 (Quantum circuits as PROPs). Our definition of QC is motivated by the fact that quantum computations typically take place in a fixed Hilbert space with each subsystem labeled. Symmetric monoidal categories with fixed types (all the objects are, say, qubits) are called PROPs [21]. We do not use this construction since we want to be able to handle also systems composed of different types of subsystems, e.g. qubits *and* qutrits.

Remark 5 (Basic notational differences to standard string diagrams). To make our presentation more approachable to readers who have a background in quantum information science (as opposed to category theory), we have decided to depart from certain common category theory conventions.

- As in standard QCDs, in the present diagrams time flows from left to right across the page. This is in contrast to the diagrams in some category theory texts in which time flows either downwards or upwards.
- In addition to the usual unit and counit morphisms η and ϵ we define the corresponding normalized states and costates: $|\cup\rangle_{\mathcal{A} \otimes \mathcal{A}} = \frac{1}{\sqrt{d}} \eta_{\mathcal{A}}$ and $\langle \cup|_{\mathcal{A} \otimes \mathcal{A}} = \frac{1}{\sqrt{d}} \epsilon_{\mathcal{A}}$, where $d = \dim \mathcal{A}$. They correspond to physically realizable entangled states and help to keep the normalization of the diagrams explicit.
- We do not use dual spaces in implementing the compact structures but rather choose a preferred *computational basis*, as is common in quantum computing. Hence our wires do not have directional markers on them.

A. Basic definitions

Remark 6 (Einstein summation convention). We make use of Einstein notation for covariant and contravariant tensor indices, along with the usual summation convention (indices appearing once as a subscript and once as a superscript in the same term are summed over) whenever the summation limits are evident from the context.

Definition 7 (Computational basis). For each d -dimensional Hilbert space \mathcal{H} we encounter we shall choose a computational basis (also called the z -basis), which we denote by $\{|i\rangle_{\mathcal{H}}\}_{i=0}^{d-1}$.

We use modulo d arithmetic for the basis vector indices, using the symbols \oplus and \ominus to denote modular addition and subtraction. When necessary, a subscript outside an operator, a ket or a bra is used to denote the subsystem it acts on or corresponds to.

Definition 8 (Discrete Fourier transform gate). We denote the discrete Fourier transform gate by H :

$$H_{\mathcal{H}} := \frac{1}{\sqrt{d}} \sum_{ab} e^{i2\pi ab/d} |a\rangle\langle b|_{\mathcal{H}}, \quad (5)$$

where $d = \dim \mathcal{H}$ is the dimension of the Hilbert space the gate acts in. We can see that $H^T = H$, and that in a qubit system H coincides with the one-qubit Hadamard gate.

Definition 9 (x -basis). Essentially the discrete Fourier transform $H_{\mathcal{H}}$ is a transformation between two mutually unbiased bases, the computational basis and the x -basis $\{|x_k\rangle_{\mathcal{H}}\}_{k=0}^{d-1}$, defined as

$$|x_k\rangle_{\mathcal{H}} := H|k\rangle_{\mathcal{H}}. \quad (6)$$

Definition 10 (Negation gate). The negation gate is defined as

$$\text{NEG}_{\mathcal{H}} := H_{\mathcal{H}}^2 = H_{\mathcal{H}}^{\dagger 2} = \sum_a |\ominus a\rangle\langle a|_{\mathcal{H}}. \quad (7)$$

As the name suggests, it performs a negation modulo d in the computational basis. As one would expect we have $\text{NEG}^2 = H^4 = \mathbb{1}$, as shown in Fig. 1. In a qubit system the negation gate reduces to the identity operator.

Definition 11 (Generalized Z and X gates). We define the generalized Z and X gates as follows [22]:

$$Z_{\mathcal{H}} := \sum_k e^{i2\pi k/d} |k\rangle\langle k|_{\mathcal{H}} \quad \text{where } d = \dim \mathcal{H}, \quad (8)$$

$$X_{\mathcal{H}} := \sum_k |k \oplus 1\rangle\langle k|_{\mathcal{H}}. \quad (9)$$

In fact the Z and X gates are the same operator in two different bases, related through conjugation with H :

$$HXH^{\dagger} = Z, \quad (10)$$

$$HZH^{\dagger} = X^{-1}. \quad (11)$$

X has the x -basis as its eigenbasis and modularly increments a computational basis state by 1, whereas Z is diagonal in the computational basis and modularly increments x -basis states:

$$\begin{aligned} X^a |k\rangle &= |k \oplus a\rangle, \\ Z^a |x_k\rangle &= HX^a H^{\dagger} H|k\rangle = H|k \oplus a\rangle = |x_{k \oplus a}\rangle. \end{aligned} \quad (12)$$

Furthermore, we have

$$Z^a X^b = e^{i2\pi ab/d} X^b Z^a \quad \text{and} \quad (13)$$

$$\text{Tr}(Z^a X^b) = d \delta_{a,0} \delta_{b,0}. \quad (14)$$

Fig. 1 presents the gate symbols we use for the Z and X gates. When \mathcal{H} is a qubit, X and Z reduce to the Pauli matrices σ_x and σ_z , respectively.

Definition 12 (Modular adder gate). We define the modular adder gate ADD as

$$\text{ADD}_{i,j} := \sum_{xy} |x, y \oplus x\rangle\langle x, y|_{i,j}. \quad (15)$$

The negated modular adder gate, NADD, is obtained by negating the ‘‘result qudit’’ of the ADD gate:

$$\text{NADD}_{i,j} := \text{NEG}_j \text{ADD}_{i,j} = \sum_{xy} |x, \ominus x \ominus y\rangle\langle x, y|_{i,j}. \quad (16)$$

In a two qubit system both ADD and NADD reduce to the CNOT gate, and thus can be understood as its generalizations. NADD is self-inverse while ADD is not, which is why we choose to use the traditional CNOT symbol to denote NADD in general. For ADD we add a small arrow to denote the output direction. Fig. 2 presents the gate symbol and identities involving ADD, NADD and H .

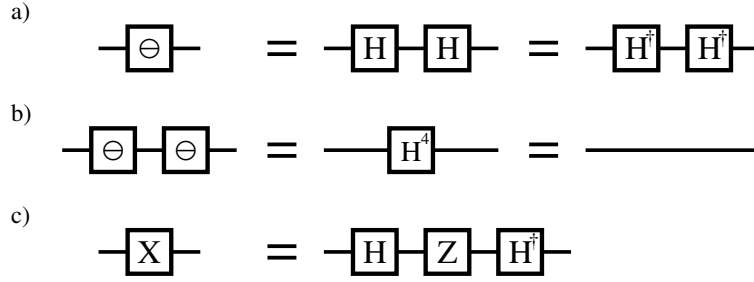


FIG. 1. Basic utility gates. (a) The NEG gate performs a modular negation in the computational basis: $\text{NEG} : |k\rangle \mapsto |\ominus k\rangle$. It can be implemented using the discrete Fourier transform gate H . (b) Negation gate squared equals identity: $\text{NEG}^2 = H^\dagger = \mathbf{1}$. (c) The X gate modularly increments by one in the computational basis: $X : |k\rangle \mapsto |k \oplus 1\rangle$. The Z gate does the same in the x -basis.

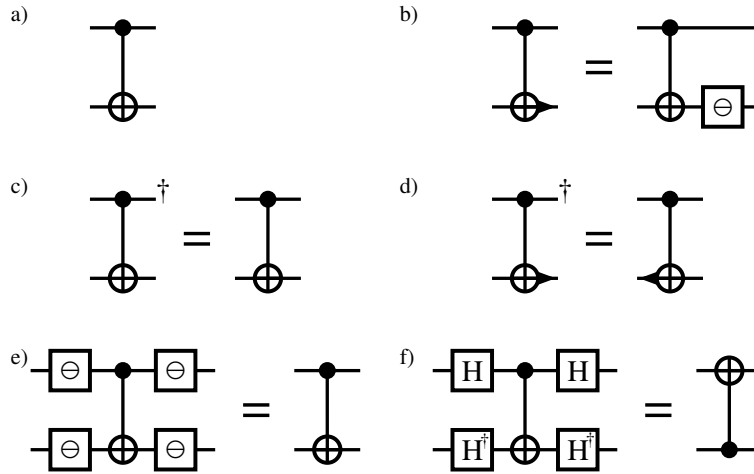


FIG. 2. (a) NADD gate: $|x, y\rangle \mapsto |x, \ominus x \oplus y\rangle$. (b) ADD gate: $|x, y\rangle \mapsto |x, x \oplus y\rangle$. (c,d) NADD is self-inverse, ADD is not, hence the need for the arrow-like symbol denoting the output direction. (e,f) Identities involving NADD, NEG and H .

Definition 13 (Generalized plus state). We define the generalized $|+\rangle_{\mathcal{H}}$ state as

$$|+\rangle_{\mathcal{H}} := |x_0\rangle_{\mathcal{H}} = H|0\rangle_{\mathcal{H}} = \frac{1}{\sqrt{d}} \sum_{i=0}^{d-1} |i\rangle_{\mathcal{H}}, \quad \text{where } d = \dim \mathcal{H}. \quad (17)$$

Definition 14 (Generalized Bell states). The concept of a Bell state, normally defined for two-qubit systems, can be generalized to systems of two d -dimensional qudits. In this case the Bell states $\{|B_{a,b}\rangle_{\mathcal{H} \otimes \mathcal{H}}\}_{a,b=0}^{d-1}$ are a set of d^2 orthonormal and maximally entangled two-qudit states. They are parameterized by two integers, a and b , and can be prepared using the Fourier and ADD gates:

$$|B_{a,b}\rangle_{\mathcal{H} \otimes \mathcal{H}} := \frac{1}{\sqrt{d}} \sum_k e^{i2\pi ak/d} |k, k \oplus b\rangle = \text{ADD}_{1,2} H_1 |a, b\rangle_{1,2}. \quad (18)$$

We will now proceed to describe the basic circuit elements appearing in the extended QCDs.

B. Systems as QC-objects

In our diagrams, much like in ordinary QCDs, time flows from left to right.² Horizontal wires each describe individual quantum systems (simple QC-objects). Stacking these wires vertically corresponds to a system comprised of several subsystems (a composite QC-object). Unless it is clear from the context, each wire should be explicitly labeled, especially if they're not all equivalent.

Alternatively, a wire A can be understood as the identity morphism 1_A . The unit object for the tensor product, $\mathbf{1}$, is represented by empty space.

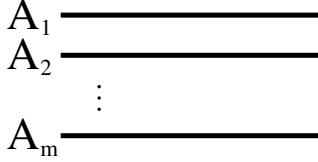


FIG. 3. Composite QC-object $A = A_1 \otimes A_2 \otimes \dots \otimes A_m$, corresponding to a system with the Hilbert space $\mathcal{A} = \mathcal{A}_1 \otimes \mathcal{A}_2 \otimes \dots \otimes \mathcal{A}_m$.

Unlike in standard QCDs, the wires are allowed to deviate from a straight horizontal line and even cross each other (which corresponds to swapping the order of the corresponding subsystems using the symmetry isomorphism c), as long as they remain *progressive* from left to right, and the relative order of the endpoints of different wires does not change. As we shall later see, a wire reversing its direction of progression has a special meaning.

C. Morphisms: states and operators on equivalent footing

Category theory allows one to study the mathematical structure formed not only by the composition of processes but also the composition of states. This becomes evident once we define both states and operators as morphisms in the category. In the diagrams the morphisms are represented by geometrical shapes connected to the wires. The one exception to this rule are morphisms of the type $f : \mathbf{1} \rightarrow \mathbf{1}$, also called *scalars*. Since the tensor unit object $\mathbf{1}$ is represented by empty space and f commutes with everything, its representation is just the number $f(1)$ anywhere in the diagram.

1. States as QC-morphisms

In QC, a pure state $|\psi\rangle_{\mathcal{A}}$ (represented by a ket, or a ray in the Hilbert space) corresponds to a linear map ψ from the unit of the tensor product $\mathbf{1}(= \mathbb{C})$ to A , or the morphism

$$\psi : \mathbf{1} \rightarrow A, \quad z \mapsto z|\psi\rangle. \quad (19)$$

For instance, consider the two-qubit state $|\Psi_+\rangle = \frac{1}{\sqrt{2}}(|01\rangle + |10\rangle)$: this corresponds to the map $\mathbb{C} \xrightarrow{\Psi_+} \mathbb{C}^2 \otimes \mathbb{C}^2$ in the category.

In a diagram a pure state (or equivalently the corresponding state preparation procedure) is represented by a left-pointing labeled triangle with a number of wires extending from its base to the right, as shown in Fig. 4. Each wire corresponds to a subsystem of the state. Flipping a triangle horizontally converts it into the corresponding costate (bra), and can be understood as a projective measurement with postselection (an *effect*).

² In converting a diagram into an algebraic expression one naturally needs to reverse the left-right order since traditional quantum mechanics uses left multiplication to represent operations on states.

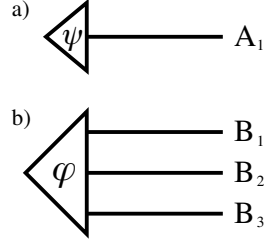


FIG. 4. (a) State $|\psi\rangle$ with a single subsystem. (b) State $|\varphi\rangle$ with three subsystems. ψ is a morphism of type $\mathbf{1} \rightarrow A_1$ and φ is a morphism of type $\mathbf{1} \rightarrow B_1 \otimes B_2 \otimes B_3$.

A state $|\psi\rangle$ can be expanded in the computational bases of its component systems, resulting in the presentation

$$|\psi\rangle = \psi^{a_1 \dots a_n} |a_1 \dots a_n\rangle_{A_1 \otimes A_2 \otimes \dots \otimes A_n}. \quad (20)$$

2. Operators as QC-morphisms

Operators, or bounded linear maps from one Hilbert space to another, can be naturally identified with the morphisms in QC. As an example we can consider quantum gates, unitary maps from a Hilbert space to itself.

In the diagrams operators are represented using labeled boxes on the wires, as shown in Fig. 5. Assume that we have a morphism $f : A \rightarrow B$, and that the domain and codomain QC-objects corresponding to tensor products of finite dimensional Hilbert spaces given by $\mathcal{A} = A_1 \otimes A_2 \otimes \dots \otimes A_m$ and $\mathcal{B} = B_1 \otimes B_2 \otimes \dots \otimes B_n$. This means that the diagram for f has m input legs and n output legs. For certain operators, such as the ADD gate, we use specific symbols.

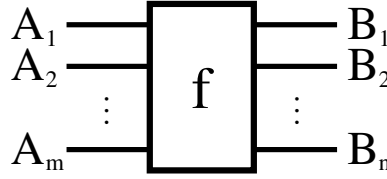


FIG. 5. Morphism $f : A \rightarrow B$, where A and B have m and n subsystems, respectively.

Using the computational bases defined on the component spaces, we can present f as

$$f = |b_1 \dots b_n\rangle \langle b_1 \dots b_n|_{\mathcal{B}} f |a_1 \dots a_m\rangle \langle a_1 \dots a_m|_{\mathcal{A}} = |b_1 \dots b_n\rangle_{\mathcal{B}} f^{b_1 \dots b_n}_{a_1 \dots a_m} \langle a_1 \dots a_m|_{\mathcal{A}}. \quad (21)$$

Given a state $|\psi\rangle_{\mathcal{A}} = \psi^{a_1 \dots a_m} |a_1 \dots a_m\rangle_{\mathcal{A}}$, we have $f|\psi\rangle_{\mathcal{A}} = f^{b_1 \dots b_n}_{a_1 \dots a_m} \psi^{a_1 \dots a_m} |b_1 \dots b_n\rangle_{\mathcal{B}}$.

3. Composition and tensor product

The category QC has two composition-like operations, the the tensor product \otimes , and the composition of morphisms \circ . The composition of morphisms is represented graphically by the sequential composition of the corresponding diagram elements and connecting the corresponding wires. Likewise, tensor products of objects or morphisms is represented by the vertical stacking of the diagram elements. These diagrammatic structures are illustrated in Fig. 6.

Remark 15 (Bifunctionality [13]). In the diagrammatic calculus, the equation

$$(g \circ f) \otimes (t \circ s) = (g \otimes t) \circ (f \otimes s) \quad (22)$$

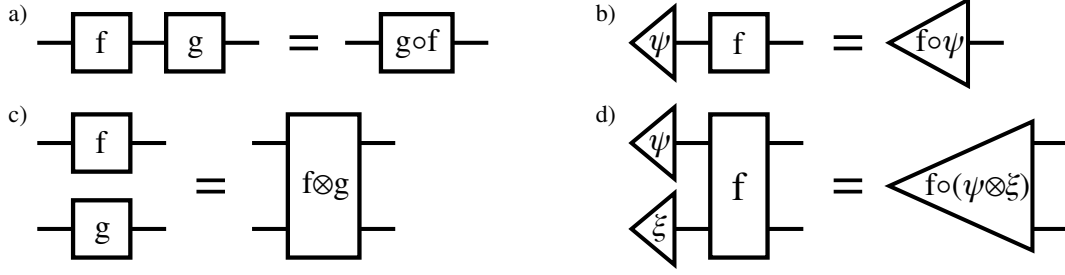


FIG. 6. Composition and tensor product. (a) Composition of operators. $(g \circ f)_c^a = g_b^a f_c^b$. (b) Composition of a state and an operator. $(f \circ \psi)_a^a = f_b^a \psi^b$. (c) Tensor product of operators. $(f \otimes g)_{b_1 b_2}^{a_1 a_2} = f_{b_1}^{a_1} g_{b_2}^{a_2}$. (d) Tensor product of states composed with an operator. $(f \circ (\psi \otimes \xi))^{a_1 a_2} = f_{b_1 b_2}^{a_1 a_2} \psi^{b_1} \xi^{b_2}$.

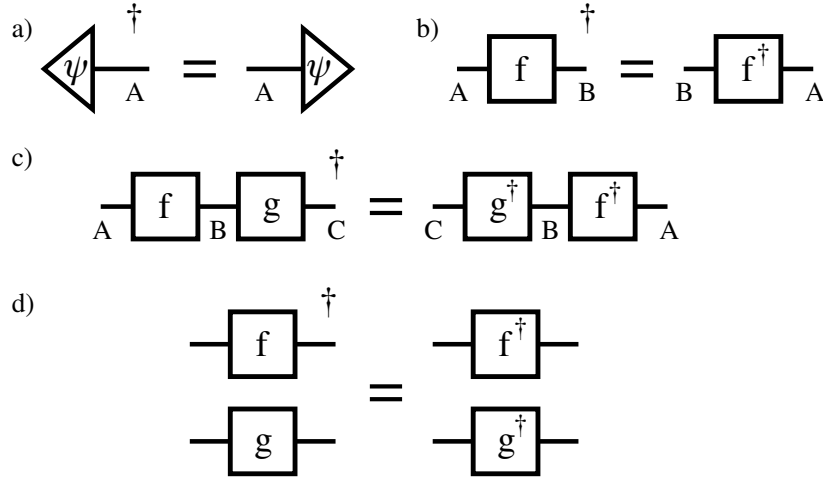


FIG. 7. Dagger functor. (a) Dagger of a state. $(\psi^\dagger)_a = \overline{\psi_a}$. (b) Dagger of an operator. $(f^\dagger)_b^a = \overline{f_b^a}$. (c) Dagger of composition. $(g \circ f)^\dagger = f^\dagger \circ g^\dagger$. (d) Dagger of tensor product. $(f \otimes g)^\dagger = f^\dagger \otimes g^\dagger$.

has the evident pictorial meaning which amounts to first connecting boxes horizontally (resulting in $g \circ f$, $t \circ s$), and then stacking them vertically to yield $(g \circ f) \otimes (t \circ s)$, or first stacking them vertically (resulting in $g \otimes t$, $f \otimes s$), and then connecting the stacks horizontally to yield $(g \otimes t) \circ (f \otimes s)$.

4. The dagger functor

The effect of the dagger functor in the category QC, taking the Hermitian conjugate of a morphism, is represented diagrammatically by mirroring the diagram in the horizontal direction. Hence given a morphism f , the diagrams corresponding to f and f^\dagger are each others' mirror images. The operator labels get a \dagger symbol appended whereas the state and costate symbols stay the same. This is illustrated in Fig. 7.

D. Cups and caps: Bell states and Bell effects

We will now make use of the structure of compact closure (see the definition of dagger-compact closure [8] as well as the more accessible read [19]) to derive elegant dualities between morphisms of different types. This provides an intuitive generalization of concepts surrounding the Choi-Jamiołkowski isomorphism.

Following ideas in [8], we introduce two new diagrammatic elements that do not appear in standard quantum circuits, shown in Fig. 8. They are the only ways a wire may reverse its direction of left-right progression.

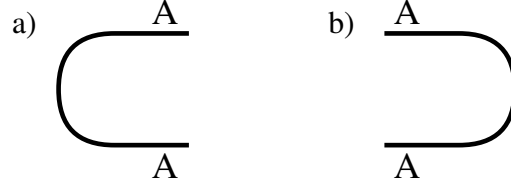


FIG. 8. Dagger-compact structures. (a) Cup η_A . (b) Cap ϵ_A .

The first one, called a *cup*, is simply another way of denoting a state preparation procedure for a generalized Bell state in the Hilbert space $\mathcal{A}^{\otimes 2}$, scaled by $\sqrt{d_A}$ where $d_A = \dim \mathcal{A}$.

Definition 16 (Cup). The cup is the diagram element that corresponds to the dagger-compact structure η of the category QC. It is a morphism $\eta_A : \mathbf{1} \rightarrow A \otimes A$, given in the computational basis as

$$\eta_A := \sum_{i=0}^{d-1} |i\rangle_{\mathcal{A}} \otimes |i\rangle_{\mathcal{A}} = \delta^{ij} |ij\rangle_{\mathcal{A} \otimes \mathcal{A}}. \quad (23)$$

It is easy to notice that η_A is proportional to the Bell state $B_{0,0}$ we defined previously:

$$|\cup\rangle_{\mathcal{A} \otimes \mathcal{A}} := |B_{0,0}\rangle_{\mathcal{A} \otimes \mathcal{A}} = \frac{1}{\sqrt{d_A}} \eta_A, \quad (24)$$

and that the other Bell states are locally equivalent to $|\cup\rangle_{\mathcal{A} \otimes \mathcal{A}}$, as shown in Fig. 9.

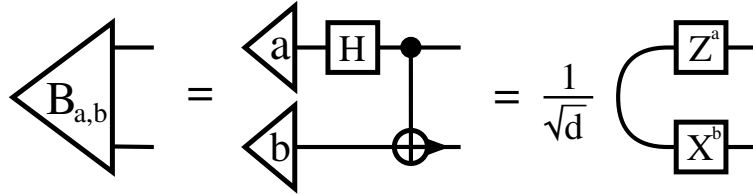


FIG. 9. Generalized Bell states. Preparation using the ADD gate, relation to the cup element.

The *cap* can be thought of physically as corresponding to a postselected measurement (an effect) in the generalized Bell basis.

Definition 17 (Cap). The cap is the diagram element that corresponds to the dagger-compact structure ϵ of the category QC. It is obtained by taking the dagger of the cup, which makes it the morphism $\epsilon_A : A \otimes A \rightarrow \mathbf{1}$:

$$\epsilon_A := \eta_A^\dagger = \sum_{i=0}^{d-1} \langle i|_{\mathcal{A}} \otimes \langle i|_{\mathcal{A}} = \delta_{ij} \langle ij|_{\mathcal{A} \otimes \mathcal{A}}. \quad (25)$$

One may safely think that the purpose of these structures is to entangle two subsystems in a way that enables very intuitive manipulation of the corresponding circuit diagrams by bending the wires in them. This is based on isomorphisms they induce between states and operators.

Now we'll demonstrate some properties of cups and caps, corresponding to the diagram identities in Fig. 10. We give proofs for cups, but corresponding identities hold for caps as well, and the proofs can be obtained by taking the Hermitian conjugates of the ones we give below.

Theorem 18 (Cup and cap symmetry (Fig. 10a)). *Since the cup corresponds to a symmetric state, it immediately follows that the relative order of the two subsystems is irrelevant. Diagrammatically this means the order of the wires can be swapped.*

Theorem 19 (Sliding operators around cups and caps (Fig. 10b)). *An operator $f : A \rightarrow B$ can be moved (“slid”) around a cup or a cap by transposing it in the computational basis. Alternatively, there is an isomorphism between a cup followed by the operator f on the first subsystem, the state $|\tilde{f}\rangle := \frac{1}{\sqrt{d_A}} \text{vec}(f^T)^k |k\rangle_{B \otimes A}$, and a cup followed by the operator f^T on the second subsystem.*³

Proof.

$$\begin{aligned} (f_j^i |i\rangle\langle j|_1) \eta_{A1,2} &= (f_j^i |i\rangle\langle j|_1) (\delta^{kl} |k\rangle_1 |l\rangle_2) = f_j^i \delta_k^j \delta^{kl} |i\rangle_1 |l\rangle_2 \\ &= f^{ij} |i\rangle_1 |j\rangle_2 = \text{vec}(f^T)^k |k\rangle_{1,2} = \sqrt{d_A} |\tilde{f}\rangle_{1,2} = f_j^i \delta_l^j \delta^{kl} |k\rangle_1 |i\rangle_2 \\ &= (f_j^i |i\rangle\langle j|_2) (\delta^{kl} |k\rangle_1 |l\rangle_2) = ((f^T)^i_j |i\rangle\langle j|_2) \eta_{B1,2} \end{aligned} \quad (26)$$

□

Corollary 20. *All local unitary operators f are isomorphic to a state $|\tilde{f}\rangle$ that is locally equivalent to a generalized Bell state.*

Corollary 21 (Conversions between inputs and outputs of the same type). *More generally, a cup converts an input leg of an operator into an output leg of same type. The opposite is true for a cap.*

Proof.

$$\begin{aligned} (f \otimes \mathbb{1}_\omega) \eta_{q,\omega} &= (|b_1 \cdots b_n\rangle \otimes |x\rangle_\omega) f^{b_1 \cdots b_n}_{a_1 \cdots a_m} \langle a_1 \cdots a_m | \otimes \langle x |_\omega \left(\delta^{kl} |k\rangle_q |l\rangle_\omega \right) \\ &= |b_1 \cdots b_n\rangle \otimes |x\rangle_\omega f^{b_1 \cdots b_n}_{a_1 \cdots a_m} \langle a_1 \cdots a_{q-1} a_{q+1} \cdots a_m | \delta^{kl} \delta^{a_q}_k \delta^{x_l} \\ &= |b_1 \cdots b_n\rangle \otimes |a_q\rangle_\omega f^{b_1 \cdots b_n}_{a_1 \cdots a_{q-1} \quad a_{q+1} \cdots a_m} \langle a_1 \cdots a_{q-1} a_{q+1} \cdots a_m | \\ &=: |b_1 \cdots b_n\rangle \otimes |a_q\rangle_\omega \hat{f}^{b_1 \cdots b_n a_q}_{a_1 \cdots a_{q-1} a_{q+1} \cdots a_m} \langle a_1 \cdots a_{q-1} a_{q+1} \cdots a_m |. \end{aligned} \quad (27)$$

□

Theorem 22 (Snake equation (Fig. 10c)). *A cup and a cap can combine to cancel each other. In other words a double bend in a wire can be pulled straight. In Section IV B we show how this operation actually corresponds to the standard quantum teleportation protocol [8].*

Proof.

$$\begin{aligned} (\epsilon_{1,2} \otimes \mathbb{1}_3) (\mathbb{1}_1 \otimes \eta_{2,3}) &= (\delta_{ij} \langle i|_1 \langle j|_2 \otimes \mathbb{1}_3) (\mathbb{1}_1 \otimes \delta^{kl} |k\rangle_2 |l\rangle_3) \\ &= \delta_{ij} \delta^{kl} \delta_k^j |l\rangle_3 \langle i|_1 = |i\rangle_3 \langle i|_1 = \mathbb{1}_{3,1}. \end{aligned} \quad (28)$$

□

Theorem 23 (Conjugate states (Fig. 10d)). *Cups and caps introduce an isomorphism between states $|\psi\rangle = \psi^k |k\rangle$ and their conjugate states $\langle \bar{\psi}| := \langle k | \psi_k$, which are obtained by complex conjugating the coefficients of the corresponding bra in the computational basis.*

Proof.

$$\langle \bar{\psi}|_2 \eta_{1,2} = (\psi_j \langle j|_2) (\delta^{kl} |k\rangle_1 |l\rangle_2) = \psi_j \delta_l^j \delta^{kl} |k\rangle_1 = \psi^k |k\rangle_1 = |\psi\rangle_1. \quad (29)$$

□

Remark 24 (Basis dependence of transposition and complex conjugation). At first it might seem strange that we should encounter basis-dependent operations such as transposition and complex conjugation. However, this is a direct result of us having chosen a preferred computational basis and defined the cup/cap operators in terms of it.

³ The vec operation takes the matrix of its operand in the computational basis and rearranges it column by column, left to right, into a column vector.

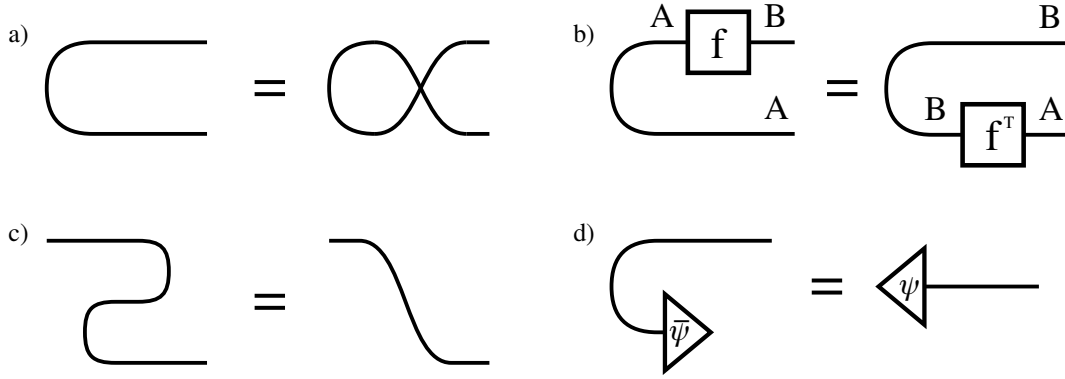
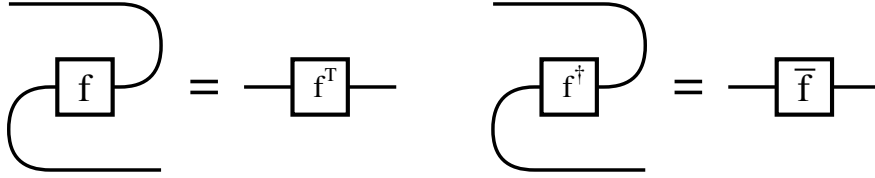


FIG. 10. Cup identities. (a) Symmetry. (b) “Sliding” an operator around a cup transposes it in the computational basis. (c) Teleportation or the “snake equation”. (d) Conjugate state.

Remark 25 (Diagrammatic adjoints). As mentioned, cups and caps allow us to take the transpose f^T of a linear map f . Following the (now) standard string diagram literature we introduce the derived concept of adjoint \bar{f} [8]:



E. Dots

Dots are a subclass of operators. Most importantly, the definition for each type of dot is trivially extensible to an arbitrary number of input and output legs, all of which have the same dimension. Dots are completely defined by their *type*, *order*, and *color*. A dot with m input legs and n output legs (an m -to- n dot) is of the order (m, n) . The color of a dot denotes the basis in which it operates. A dot of the order (m, n) , operating in the basis B is denoted as $\text{DOT}_B^{m \rightarrow n}$. In the diagrams dots are represented by a circular node (“dot”) with a symbol denoting the type of the dot and a label denoting the color.

Definition 26 (General properties of dots).

- All dots are by definition symmetric both in their inputs and their outputs.
- The dagger functor simply converts a dot’s input legs into output legs and vice versa:

$$\text{DOT}_B^{m \rightarrow n\dagger} = \text{DOT}_B^{n \rightarrow m}. \quad (30)$$

- The unitary transformation from the computational basis to the orthonormal basis $B = \{|b_k\rangle\}_k$, $U_B := \sum_k |b_k\rangle\langle k|$, can be used to convert a general DOT_B into a DOT_z :

$$\text{DOT}_B^{m \rightarrow n} = U_B^{\otimes n} \text{DOT}_z^{m \rightarrow n} U_B^{\dagger \otimes m}. \quad (31)$$

These properties are illustrated in Fig. 11.

Definition 27 (Unit element). A *unit element* for a dot of a given type and color is a state/costate which, when connected to a leg of the dot eliminates that leg, reducing the corresponding order of the dot by one.

$$\begin{aligned} \text{DOT}^{m \rightarrow n} |\text{unit}\rangle &= \text{DOT}^{(m-1) \rightarrow n}, \\ \langle \text{unit} | \text{DOT}^{m \rightarrow n} &= \text{DOT}^{m \rightarrow (n-1)}. \end{aligned} \quad (32)$$

Now we will introduce specific types of dots.

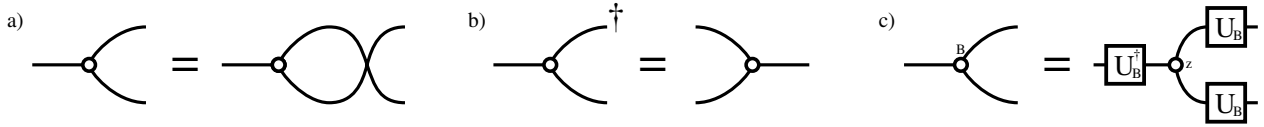


FIG. 11. Dots. We use a generic 1-to-2 dot as an example, but these properties apply to dots of all types, orders and colors. (a) Symmetry. (b) Dagger reverses the order but preserves the type of a dot. (c) Transformation between dots of different colors. $U_B = \sum_k |b_k\rangle\langle k|$.

1. Copy dots

Definition 28 (COPY). We define the m -to- n copy dot in the computational basis as

$$\text{COPY}_z^{m \rightarrow n} := \sum_k |k \cdots k\rangle_n \langle k \cdots k|_m. \quad (33)$$

In our diagrammatic notation a copy dot is represented by a circular node with the symbol $=$ inside, and a label identifying the basis. Connecting a basis state $|k\rangle$ (or the corresponding costate) to any of the legs of the copy dot collapses the sum and breaks the dot up into unconnected copies of $|k\rangle$ and $\langle k|$. For example the 1-to-2 copy dot

$$\text{COPY}_B^{1 \rightarrow 2} = \sum_k |b_k b_k\rangle \langle b_k|, \quad (34)$$

given the state $|b_k\rangle$ as the input, produces two copies of the same state as output. ⁴ Fig. 12 depicts this in diagram form.

As a special case, to conform with the standard quantum circuit notation, the copy dot in the computational basis is represented by a simple black dot \bullet .

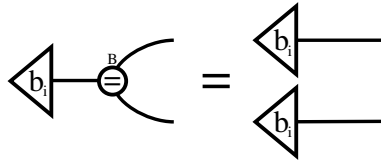


FIG. 12. Copy dot $\text{COPY}_B^{1 \rightarrow 2}$ in the orthonormal basis $B = \{|b_k\rangle\}_k$.

Remark 29 (COPY as a quantum operation). Direct calculation gives

$$\text{COPY}_B^{m \rightarrow n \dagger} \text{COPY}_B^{m \rightarrow n} = \sum_i |b_i \cdots b_i\rangle_m \langle b_i \cdots b_i|_m = \mathbb{1} \quad \Leftrightarrow \quad m = 1. \quad (35)$$

Hence an m -to- n copy dot is a valid quantum operation iff $m = 1$. This property is not preserved under the dagger — $\text{COPY}_B^{1 \rightarrow n \dagger} = \text{COPY}_B^{n \rightarrow 1}$ (*merge*) is not a valid quantum operation if $n > 1$. It is however still useful to consider its properties — by invoking arguments such as postselection it can be given a physical meaning.

⁴ This does not violate the no cloning theorem since the operator can only faithfully copy a single fixed basis.

2. Plus dots

Definition 30 (PLUS). We define the m -to- n plus dot in the computational basis as

$$\begin{aligned} \text{PLUS}_z^{m \rightarrow n} &:= H^{\otimes n} \text{COPY}_z^{m \rightarrow n} H^{\otimes m} = \text{COPY}_x^{m \rightarrow n} \text{NEG}^{\otimes m} \\ &= \frac{1}{d^{(m+n-2)/2}} \sum_{\substack{x_1 \cdots x_m \\ y_1 \cdots y_n}} \delta_{(\sum_i x_i \oplus \sum_j y_j), 0} |y_1 \cdots y_n\rangle \langle x_1 \cdots x_m|, \end{aligned} \quad (36)$$

where d is the dimension of the legs.

Roughly speaking the plus dot makes sure all its inputs and outputs in the given basis sum to zero mod d . The plus dot is generally not a copy dot. Diagrammatically a plus dot is represented by a circular node with a plus symbol inside, and a label identifying the basis. Again, to conform with the standard quantum circuit notation, PLUS_z is represented simply by the symbol \oplus .⁵

3. Spider law

Neighboring copy dots of the same color B can be merged into a single dot. In categorical quantum mechanics, this is called the spider law.

Theorem 31 (Spider law [17]). *Given a connected graph with m inputs and n outputs comprised solely of copy dots of the same color (and dimension), this map can be equivalently expressed as a single m -to- n dot, as shown in Fig. 13.*

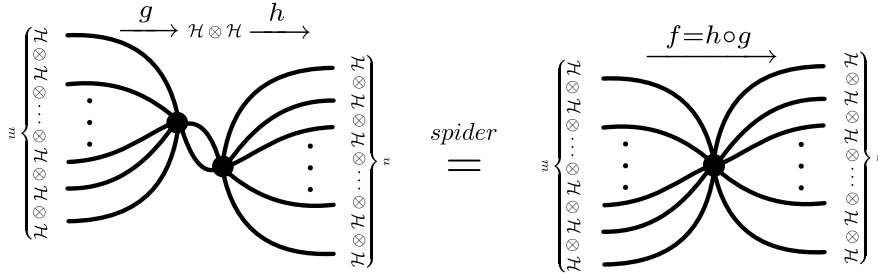


FIG. 13. Spider law.

The plus dots obey a slightly modified version of the spider law, in which all the connecting legs between two dots to be merged must have the negation gate $\text{NEG}_B := U_B \text{NEG} U_B^\dagger$ on them.

4. Simplification rules

It is easy to see that $\sqrt{d}|0\rangle$ is a unit element for PLUS_z since it simply makes the corresponding index vanish in the Kronecker delta in Eq. (36). Using this result it is straightforward to show that $\sqrt{d}|+\rangle$ is a unit element for COPY_z . The interaction of the unit elements with their dots is presented in Fig. 14.

Remark 32 (Induced dagger-compact structures). Three legged dots induce compact structures whenever there is a state or costate that, when connected to a leg of the dot, transforms it to a state locally equivalent to a cup or a cap.

⁵ The diagrammatic representation of $\text{PLUS}_z^{1 \rightarrow 1}$ (a wire with \oplus on it) must not be confused with the notation occasionally used in standard QCDs, in which \oplus denotes the NOT gate. In our notation we instead have $\text{PLUS}_z^{1 \rightarrow 1} = \text{NEG}$. Following this logic we could have used \oplus as the symbol of the NEG gate as well but felt this notational parsimony would not have been worth the potential confusion.

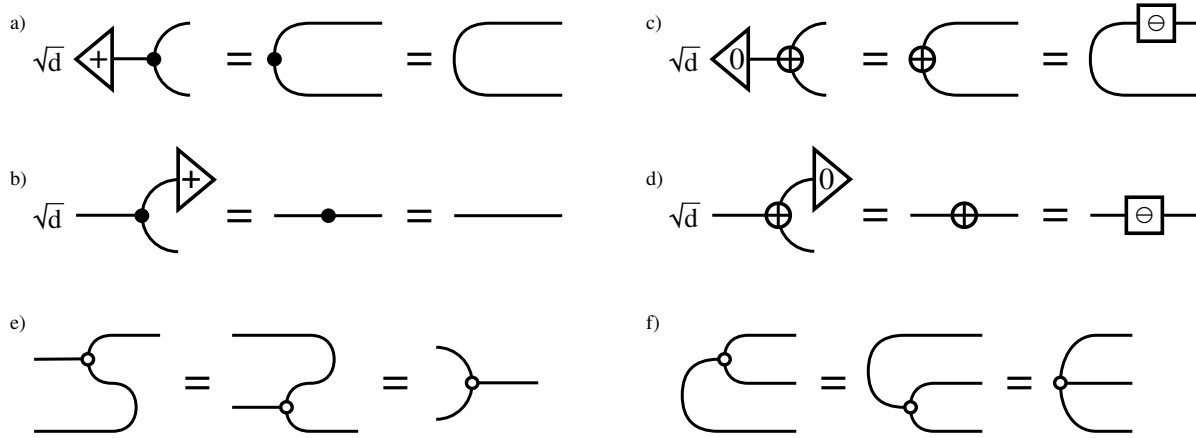


FIG. 14. Unit elements for the (a,b) \bullet and (c,d) \oplus dots. (e,f) Bending the legs of copy and plus dots using cups and caps. Here the empty dot refers to any copy or plus dot for which $U_B = \overline{U_B}$, e.g. the \bullet and \oplus dots.

Theorem 33 (Bending the legs of dots). *The effect of attaching a cup to an input leg of a copy or plus dot of any color for which $U_B = \overline{U_B}$ is to change it into an output leg. The same is of course true under the dagger.*

$$\text{COPY}_z^{m \rightarrow n} \eta = \text{COPY}_z^{(m-1) \rightarrow (n+1)}, \quad (37)$$

$$\epsilon \text{ COPY}_z^{m \rightarrow n} = \text{COPY}_z^{(m+1) \rightarrow (n-1)}. \quad (38)$$

This is illustrated in Fig. 14(e,f).

Theorem 34 (Commutation rules for the Z and X gates with dots). *Since the Z gate shares an eigenbasis with COPY_z , they fully commute:*

$$\sum_k |k\rangle_1 |k\rangle_2 \langle k|_1 Z = \sum_k (Z|k\rangle_1) |k\rangle_2 \langle k|_1 = \sum_k |k\rangle_1 (Z|k\rangle_2) \langle k|_1. \quad (39)$$

The X gate, however, is multiplied when it passes a COPY_z :

$$\sum_k |k\rangle_1 |k\rangle_2 \langle k|_1 X = \sum_k |k\rangle_1 |k\rangle_2 \langle k \oplus 1|_1 = \sum_k |k \oplus 1\rangle_1 |k \oplus 1\rangle_2 \langle k|_1 = \sum_k (X|k\rangle_1) (X|k\rangle_2) \langle k|_1 \quad (40)$$

One obtains equivalent results for PLUS_z with the roles of Z and X exchanged. These commutation rules are presented in Fig. 15. Even though we used $1 \rightarrow 2$ dots in our proofs above, analogous rules apply to COPY_z and PLUS_z dots with an arbitrary number of legs.⁶

Now we have assembled all the necessary ingredients to make the dots do something useful. As the astute reader probably already has noticed, the notation we use for the \bullet and \oplus dots is suggestively similar to the NADD gate symbol, for a good reason. Fig. 16 shows how the NADD gate can be built out of dots, and how the \bullet and \oplus dots can be in some cases explicitly constructed using the NADD gate.

⁶ Aesthetic interlude: Given the computational basis, the set of operations $\{1, T, \bar{\cdot}, \dagger\}$ is isomorphic to the Klein group $Z_2 \times Z_2$, which also is the symmetry group of the rectangle. We can use this to illustrate the symmetry properties of operators with the symbols, by equating T with a 180-degree rotation of the symbol, $\bar{\cdot}$ with vertical reflection, and \dagger with horizontal reflection. (This is analogous to the function of the corner marker on the morphism symbols in [12].) By adding an arrow to the X gate symbol to denote the direction of incrementation, together with the symmetries of the letter symbols themselves, we can see that the symmetry properties of the Z and X gates are exactly represented by the symmetries of their gate symbols: $Z^T = Z$, $\overline{X} = X$. The arrow would not be necessary if the symbol for the X gate had the correct symmetry in itself (like the letter E , for example), but we chose to go with the more traditional symbol.

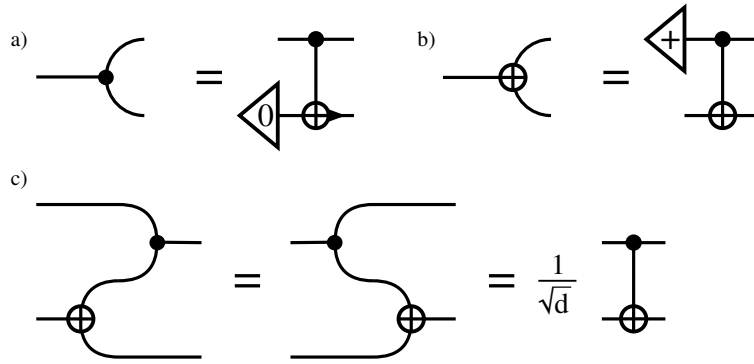
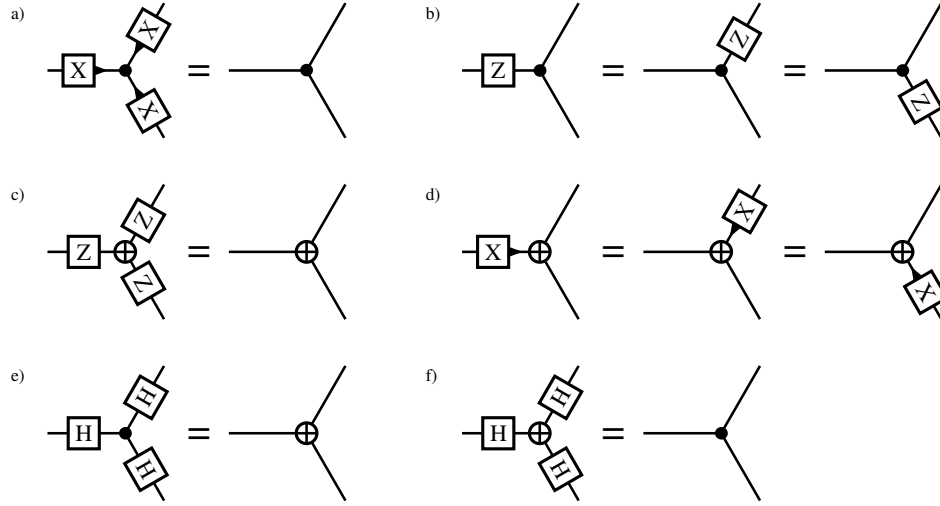


FIG. 16. (a–b) Explicit constructions for the • and ⊕ dots. (c) Combining the • and ⊕ dots yields NADD.

5. Bialgebra law

Theorem 35 (Bialgebra law). *Two NADD gates connected to each other via a SWAP gate as in Fig. 17 are equal to a single inverted NADD gate.*

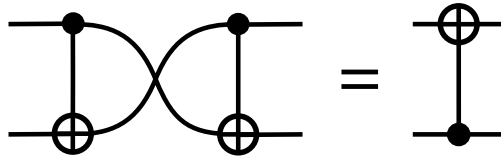


FIG. 17. Bialgebra law.

Proof.

$$\begin{aligned}
 \text{NADD}_{1,2}\text{SWAP}_{1,2}\text{NADD}_{1,2} &= \sum_{abxy} |x, \ominus x \ominus y\rangle_{1,2} \langle y, x | a, \ominus a \ominus b \rangle \langle a, b |_{1,2} \\
 &= \sum_{ab} | \ominus a \ominus b, b \rangle \langle a, b |_{1,2} = \text{NADD}_{2,1}.
 \end{aligned} \tag{41}$$

□

F. From diagrams to quantum operations

The extended QCDs each correspond to a QC-morphism. However, not every such morphism is physically implementable on its own. In quantum mechanics a state operator can (in principle) undergo any evolution that can be expressed as a linear, completely positive map (CPM). The mapping from QC-morphisms to CPMs is easiest achieved using the operator-sum representation, in which each morphism corresponds to a Kraus operator.

Definition 36 (Complete set of QC-morphisms). We call a set of QC-morphisms $S = \{f_i\}_i \subset \text{hom}_{\text{QC}}(A, B)$ *complete* iff it corresponds to a quantum operation, that is,

$$S \text{ is complete} \Leftrightarrow \sum_i f_i^\dagger f_i = \mathbb{1}_A. \quad (42)$$

The effect of S on the state operator $\rho : A \rightarrow A$ is

$$\rho \mapsto \sum_i f_i \rho f_i^\dagger. \quad (43)$$

Another category-based approach to representing CPMs using diagrams can be found in [23].

Lemma 37 (Properties of complete sets of QC-morphisms). *The following properties immediately follow from the definition:*

- (a) If $f : A \rightarrow A$ is unitary, it is complete on its own.
- (b) A state $\psi : \mathbf{1} \rightarrow A$ is complete on its own iff it is normalized: $\langle \psi | \psi \rangle = 1$.
- (c) A set of costates $\{\chi_k : A \rightarrow \mathbf{1}\}_k$ is complete if the corresponding states form an orthonormal basis for A : $\sum_k |\chi_k\rangle \langle \chi_k|_A = \mathbb{1}_A$. In this case the set of costates corresponds to a projective measurement in this basis.
- (d) If $\{f_i\}_i \subset \text{hom}_{\text{QC}}(A, B)$ and $\{g_j\}_j \subset \text{hom}_{\text{QC}}(C, D)$ are complete sets of morphisms, the tensor product set $\{f_i \otimes g_j\}_{ij}$ is also complete.
- (e) If $\{f_i\}_i \subset \text{hom}_{\text{QC}}(A, B)$ and $\{g_j\}_j \subset \text{hom}_{\text{QC}}(B, C)$ are complete sets of morphisms, the composited set $\{g_j \circ f_i\}_{ij}$ is also complete.

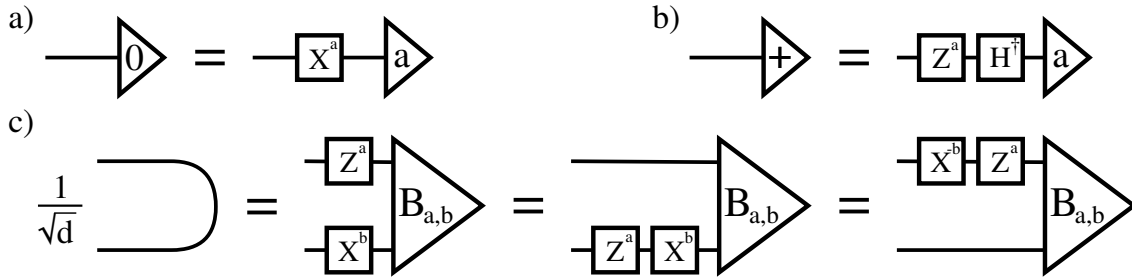


FIG. 18. Representations of the (a) $\langle 0|$ and (b) $\langle +|$ costates and (c) caps in terms of complete sets of costates with local corrections. The generalized Bell costates $\langle B_{a,b}|$ can be presented in terms of computational basis costates e.g. using the inverse of the circuit in Fig. 9.

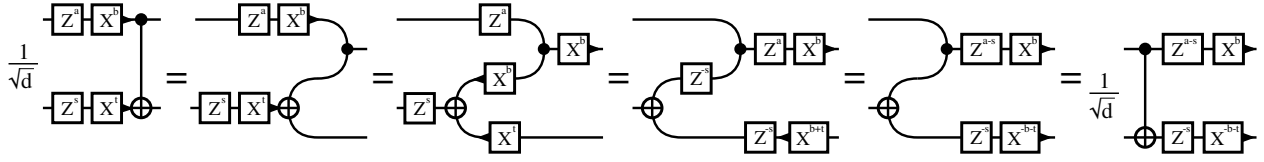
In constructing complete sets of QC-morphisms it is useful to be able to implement caps and certain other costates in terms of projective measurements followed by local unitary corrections dependent on the outcome. This can be done by first expressing the costate in terms of a complete set of standard basis costates (as shown in Fig. 18) and then using Theorem 19 together with commutation rules between various circuit elements and the Z and X gates. In the computational basis $Z^T = Z$ and $X^T = X^{-1}$, so they both can readily be slid around cups and caps. By shuttling them along the circuit to positions which causally follow the costate that introduced them (if possible!), the circuit becomes physically implementable. Examples on how this is accomplished in practice are given in the next section.

IV. APPLICATIONS

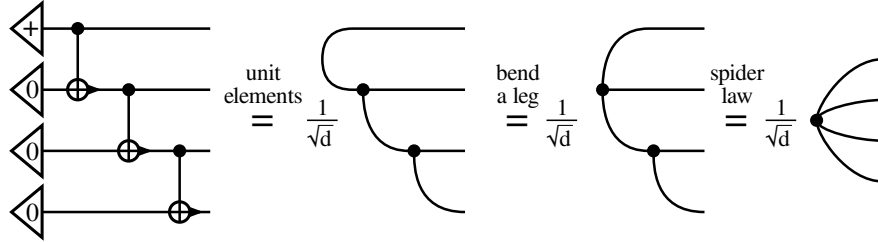
Here we present some applications of the extended quantum circuit diagram methods derived in the last section. First we give some examples of circuit simplification, and then derive several well-known quantum protocols for systems of arbitrary dimension using almost no algebra beyond what is implicit in the diagrams.

A. Circuit simplification

Example 38 (Commuting Z and X gates through a NADD gate). Start by breaking the NADD gate into a copy dot and a plus dot as shown in Fig. 16. Then apply the commutation rules presented in Fig. 15 to commute the Z and X gates through the dots one by one, and finally put the NADD gate together again. The result is the d -dimensional generalization of the familiar commutation rules between σ_z , σ_x and a CNOT.



Example 39 (GHZ circuit). We are given the d -dimensional version of the standard circuit for preparing Greenberger-Horne-Zeilinger (GHZ) states. We start by breaking up the ADD gates into \bullet and \oplus dots as shown in Fig. 16(c), then apply the unit element identities in Fig. 14 (or alternatively use the dot constructions in Fig. 16(a,b) in reverse) to obtain a network of copy dots and cups. We use the cups to bend the input legs of the copy dots into output legs, and finally invoke the spider law to fuse the copy dots together:

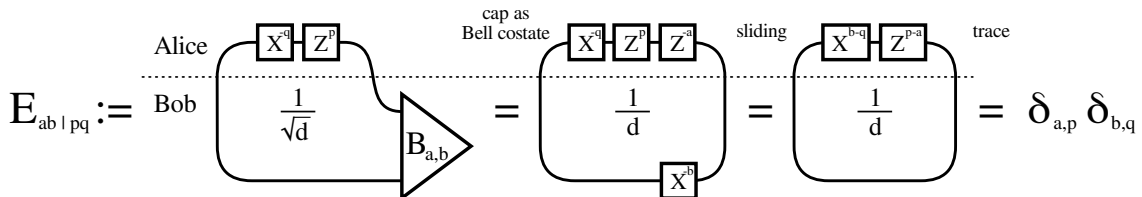


The result is a scaled $\text{COPY}_z^{0 \rightarrow 4}$ dot, which is equal to the four-qudit GHZ state as expected:

$$\frac{1}{\sqrt{d}} \text{COPY}_z^{0 \rightarrow 4} = \frac{1}{\sqrt{d}} \sum_k |kkkk\rangle = |\text{GHZ}_4\rangle. \quad (44)$$

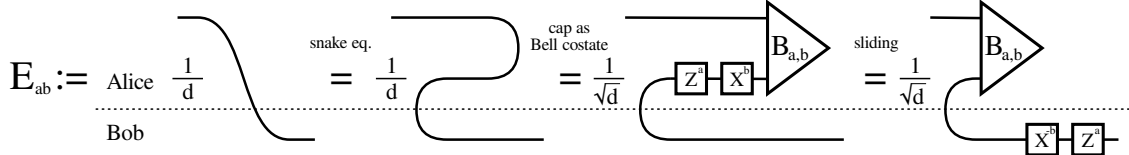
B. Quantum protocols

Example 40 (Superdense coding). We start with a diagram representing a cup state followed by local operation $Z^p X^{-q}$ by Alice, and finally a Bell measurement with the outcome (a, b) by Bob. We then express the Bell costate using a cap and Z and X gates, slide the gates around the bends and obtain a trace expression which is easily evaluated using Eq. (14).



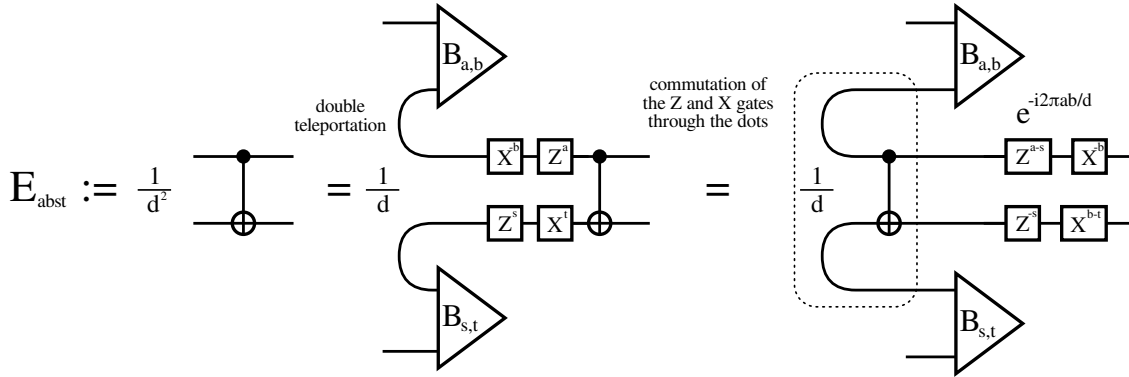
The corresponding Kraus operators are $E_{ab|pq} = \delta_{a,p}\delta_{b,q}$. This set of morphisms is complete for all possible local operations (p, q) . Furthermore, the probability of Bob obtaining the measurement outcome (a, b) is $P_{ab} = \text{Tr}(E_{ab|pq}\rho E_{ab|pq}^\dagger) = \delta_{a,p}\delta_{b,q} \text{Tr}(\rho) = \delta_{a,p}\delta_{b,q}$. Hence the result of Bob's measurement is completely determined by Alice, and she use this protocol to can transmit two d-its worth of information to Bob.

Example 41 (Teleportation [24]). Using the snake equation, expressing the cap in terms of a Bell costate preceded by Z and X gates, and sliding the gates around the cup, we obtain a causal diagram that represents the (a, b) outcome of a Bell measurement by Alice, followed by local corrections dependent on the measurement result by Bob.



The corresponding Kraus operators are $E_{ab} = \frac{1}{d}\mathbb{1}$ for all a, b . This set of morphisms is easily seen to be complete. Together these diagrams must represent a physical operation, $\rho \mapsto \sum_{ab} E_{ab}\rho E_{ab}^\dagger = \rho$, which faithfully transports any quantum state ρ from Alice to Bob.

Example 42 (Teleportation through a gate [25]). Starting from a two-qudit gate (NADD in our example), we use the teleportation protocol once for each input qudit, commute the local Z and X corrections through the NADD as in Example 38, and finally regroup the gates.



The resulting diagrams each correspond to the same NADD gate operation and form a complete set. This allows us to implement any gate U in an atemporal order: First we apply the gate to a number of cup states, obtaining the state $|\bar{U}\rangle$ (inside the dotted line in the diagram), isomorphic to U . The inputs are then teleported “through” the gate-state, effectively applying U on them, even if they did not even exist yet when the gate was actually used. Furthermore, the states $|\bar{U}\rangle$ can be prepared beforehand in large numbers and used only when needed. This is useful e.g. in the case where the success of an individual U operation is not guaranteed, but the computation itself must not fail.

V. CONCLUSION

We have provided an explicit representation of dagger compact closed categories in terms of the quantum circuit model. Using the corresponding string diagram calculus, the language of quantum circuit diagrams was extended in a way that enables powerful new ways of manipulating and simplifying circuits of systems of arbitrary dimension, while remaining within a framework that is directly and easily applicable to problems stated in the language of quantum information science. We hope the present paper will lead to many new research directions in quantum information science, for both physicists and those working in applied mathematics. In particular, our approach has further applications in applying category theory and related ideas to tensor network simulation, as was initiated in recent work [11].

ACKNOWLEDGMENTS

We thank Samson Abramsky and John Baez. JDB received support from EPSRC grant EP/G003017/1. VB visited Oxford using funding from this same grant. JDB completed large parts of this work visiting the Center for Quantum Technologies, at the National University of Singapore (this visit was hosted by Vlatko Vedral).

Appendix A: Uniqueness of the cup state

Assume that given the Hilbert spaces A and A' , we can write down two bipartite states

$$|\psi_1^A\rangle = c_{xy}|x\rangle_A|y\rangle_B, \quad (\text{A1})$$

$$|\psi_2^{A'}\rangle = d_{xy}|x\rangle_{A'}|y\rangle_{B'} \quad (\text{A2})$$

that should play the role of the cup, where the complex coefficients c_{xy} and d_{xy} can be interpreted as elements of the matrices C and D . The normalization condition gives

$$\langle\psi_1|\psi_1\rangle = c_{xy}^*c_{xy} = \text{Tr}(C^\dagger C) = 1, \quad (\text{A3})$$

$$\langle\psi_2|\psi_2\rangle = d_{xy}^*d_{xy} = \text{Tr}(D^\dagger D) = 1. \quad (\text{A4})$$

We require that the pair of states should have the following property: For every linear operator

$$f : A \rightarrow A', \quad f = f_{ij}|i\rangle_{A'}\langle j|_A$$

there is another linear operator

$$g : B \rightarrow B', \quad g = g_{ij}|i\rangle_{B'}\langle j|_B$$

and vice versa such that the graphical equality in Fig. 19 holds; we want to be able to “slide” the operators around the cup. For the sliding operation to make sense, the dimensions of the external legs must remain the same.

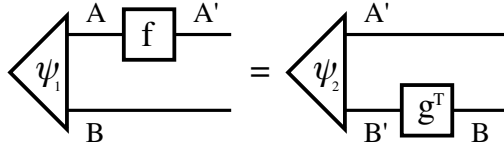


FIG. 19. “Sliding” linear operators around a cup state.

In equation form this is

$$\begin{aligned} f_{ij}c_{xy}|i\rangle_{A'}\langle j|x\rangle_A|y\rangle_B &= f_{ij}c_{jy}|i\rangle_{A'}|y\rangle_B = f_{ij}c_{jk}|i\rangle_{A'}|k\rangle_B \\ &= (g^T)_{ij}d_{xy}|x\rangle_{A'}\langle j|y\rangle_{B'}|i\rangle_B = d_{xj}g_{ji}|x\rangle_{A'}|i\rangle_B = d_{ij}g_{jk}|i\rangle_{A'}|k\rangle_B, \end{aligned} \quad (\text{A5})$$

which is equivalent to the matrix equation

$$FC = DG. \quad (\text{A6})$$

Now let us apply the singular value decomposition on C and D . SVD is given by $X = U\Sigma V^\dagger$, where U and V^\dagger are unitary and Σ is a diagonal matrix with the (real, nonnegative) singular values σ_k of X on the diagonal in descending order. We obtain

$$\begin{aligned} F(U_C\Sigma_C V_C^\dagger) &= (U_D\Sigma_D V_D^\dagger)G \\ \Leftrightarrow (U_D^\dagger F U_C)\Sigma_C &= \Sigma_D(V_D^\dagger G V_C) \\ \Leftrightarrow \tilde{F}\Sigma_C &= \Sigma_D\tilde{G}. \end{aligned} \quad (\text{A7})$$

The state normalization condition is equivalent to $\sum_k \sigma_k^2 = 1$. Thus for both C and D we always have $\sigma_1 > 0$. Comparing the elements $(\dim A', 1)$ and $(1, \dim B)$ on both sides we find that unless $\dim A \geq \dim B$, $\dim A' \leq \dim B'$, $\sigma_{C \dim B} > 0$ and $\sigma_{D \dim A'} > 0$, there are either matrices F for which there is no G such that Eq. (A6) holds, or vice versa.

Now assume we wish to impose two additional constraints: The cup states have to be symmetric and map unitary operators to unitary operators. The first constraint gives $A \cong B$ and $A' \cong B'$, which means that Σ_C and Σ_D are both square and, since their singular values are all positive, invertible:

$$\tilde{G} = \Sigma_D^{-1} \tilde{F} \Sigma_C \Leftrightarrow G = D^{-1} F C. \quad (\text{A8})$$

Furthermore, for every unitary matrix \tilde{F} we must have

$$\tilde{G} \tilde{G}^\dagger = \Sigma_D^{-1} \tilde{F} \Sigma_C \Sigma_C^\dagger \tilde{F}^\dagger (\Sigma_D^{-1})^\dagger = \Sigma_D^{-1} \tilde{F} \Sigma_C^2 \tilde{F}^\dagger \Sigma_D^{-1} = \mathbb{1} \Leftrightarrow \tilde{F} \Sigma_C^2 = \Sigma_D^2 \tilde{F}. \quad (\text{A9})$$

Now Schur's Lemma for unitary representations of Lie groups says that Σ_C and Σ_D must both be scalar multiples of identity. Together with the normalization condition this completely fixes the singular values, and we can choose $C = \frac{1}{\sqrt{d_A}} U$ and $D = \frac{1}{\sqrt{d_{A'}}} V$, where U and V are symmetric unitary matrices. Thus

$$|\psi_1^A\rangle = c_{xy} |x\rangle_A |y\rangle_A = \frac{1}{\sqrt{d_A}} U_{xy} |x\rangle_A |y\rangle_A = (U \otimes \mathbb{1}) |\cup\rangle_{A \otimes A}, \quad (\text{A10})$$

and the most general cup state for the Hilbert space $A \otimes A$ is a local unitary rotation of $|\cup\rangle_{A \otimes A}$.

- [1] A. C.-C. Yao, in *Proc. of the 34th Ann. Symp. on Foundations of Computer Science* (IEEE Computer Society, 1993) pp. 352–361, ISBN 0-8186-4370-6.
- [2] D. Aharonov, A. Kitaev, and N. Nisan, in *STOC '98: Proceedings of the thirtieth annual ACM symposium on Theory of computing* (ACM, 1998) pp. 20–30, arXiv:quant-ph/9806029.
- [3] A. Barenco, D. Deutsch, A. Ekert, and R. Jozsa, *Phys. Rev. Lett.* **74**, 4083 (1995), arXiv:quant-ph/9503017.
- [4] A. Barenco, C. H. Bennett, R. Cleve, D. P. DiVincenzo, N. Margolus, P. Shor, T. Sleator, J. A. Smolin, and H. Weinfurter, *Phys. Rev. A* **52**, 3457 (1995), arXiv:quant-ph/9503016.
- [5] A. Kitaev, A. Shen, and M. Vyalyi, *Classical and quantum computation*, Graduate Studies in Mathematics, Vol. 47 (AMS, 2002) see also [26].
- [6] J. C. Baez and M. Stay, “Physics, Topology, Logic and Computation: A Rosetta Stone,” (Mar. 2009), arXiv:0903.0340 [quant-ph].
- [7] J. C. Baez and A. Lauda, “A Prehistory of n-Categorical Physics,” (Aug. 2009), arXiv:0908.2469 [hep-th].
- [8] S. Abramsky and B. Coecke, “Handbook of quantum logic and quantum structures,” (Elsevier, 2008) Chap. Categorical quantum mechanics, arXiv:0808.1023.
- [9] D. Gross, J. Eisert, N. Schuch, and D. Perez-Garcia, *Phys. Rev. A* **76**, 052315 (Nov. 2007), arXiv:0706.3401 [quant-ph].
- [10] R. B. Griffiths, S. Wu, L. Yu, and S. M. Cohen, *Phys. Rev. A* **73**, 052309 (May 2006), arXiv:quant-ph/0507215.
- [11] J. Biamonte, S. R. Clark, and D. Jaksch, *Algebra and Coalgebra on Categorical Tensor Network States*, Tech. Rep. RR-10-14 (OUCL, 2010).
- [12] P. Selinger, “A survey of graphical languages for monoidal categories,” (Aug. 2009), arXiv:0908.3347 [math.CT].
- [13] A. Joyal and R. Street, *Advances in Mathematics* **88**, 55 (1991).
- [14] S. Mac Lane, *Categories for the Working Mathematician (Graduate Texts in Mathematics)*, 2nd ed. (Springer, 1998) ISBN 0387984038.
- [15] Y. Lafont, *Journal of Pure and Applied Algebra* **184**, 257 (2003).
- [16] Y. Guiraud, *Annals of Pure and Applied Logic* **141**, 266 (2006), arXiv:math/0612089.
- [17] B. Coecke and R. Duncan, “Interacting quantum observables: Categorical algebra and diagrammatics,” (2009), arXiv:0906.4725.
- [18] B. Coecke, *Contemporary Physics* **51**, 59 (2010), arXiv:0908.1787.
- [19] B. Coecke, in *AIP Conference Proceedings*, Vol. 810 (AIP, 2006) pp. 81–98, arXiv:quant-ph/0510032.
- [20] S. Abramsky and B. Coecke, in *Proceedings of the 19th Annual IEEE Symposium on Logic in Computer Science* (2004) pp. 415–425.
- [21] S. Mac Lane, *Bull. Amer. Math. Soc.* **71**, 40 (1965).
- [22] L. Roa, A. Delgado, and I. Fuentes-Guridi, *Phys. Rev. A* **68**, 022310 (Aug 2003), arXiv:quant-ph/0304002.
- [23] P. Selinger, *Electronic Notes in Theoretical Computer Science* **170**, 139 (2007), proceedings of the 3rd International Workshop on Quantum Programming Languages (QPL 2005).

- [24] C. H. Bennett, G. Brassard, C. Crépeau, R. Jozsa, A. Peres, and W. K. Wootters, *Phys. Rev. Lett.* **70**, 1895 (Mar 1993).
- [25] D. Gottesman and I. L. Chuang, *Nature* **402**, 390 (1999), arXiv:quant-ph/9908010.
- [26] D. Aharonov and T. Naveh, “Quantum NP—a survey,” (2002), arXiv:quant-ph/0210077.